ACS APPLIED MATERIALS & INTERFACES

Research Article

www.acsami.org

MT1-MMP Responsive Doxorubicin Conjugated Poly(lactic-*co*-glycolic Acid)/Poly(styrene-*alt*-maleic Anhydride) Core/Shell Microparticles for Intrahepatic Arterial Chemotherapy of Hepatic Cancer

Enkhzaya Davaa,[†,#] Junghan Lee,[†,#] Ratchapol Jenjob,[‡] and Su-Geun Yang*[,†]

[†]Department of New Drug Development, School of Medicine, Inha University, B-308, Chungsuk Bldg, 366, Seohae-Daero, Jung-Gu, Incheon 22332, Republic of Korea

[‡]Department of Materials Science and Engineering, School of Molecular Science and Engineering, Vidyasirimedhi Institute of Science and Technology (VISTEC), Rayong 21210, Thailand

Supporting Information

ABSTRACT: In this study, we demonstrated that the MT1-MMP-responsive peptide (sequence: GPLPLRSWGLK) and doxorubicin-conjugated poly(lactic-*co*-glycolic acid/poly-(styrene-*alt*-maleic anhydride) core/shell microparticles (PLGA/pSMA MPs) can be applied for intrahepatic arterial injection for hepatocellular carcinoma (HCC). PLGA/pSMA MPs were prepared with a capillary-focused microfluidic device. The particle size, observed by scanning electron microscopy (SEM), was around 22 ± 3 μm. MT1-MMP-responsive peptide and doxorubicin (DOX) were chemically conjugated with pSMA segments on the shell of MPs to form a PLGA/pSMA-peptide-DOX complex, resulting in high encapsulation efficiency (91.1%) and loading content (2.9%). DOX was released from PLGA/pSMA-peptide-DOX MPs in a pH-dependent manner (~25% at pH 5.4 and ~8% at pH 7.4) and accumulated significantly in an MT1-MMP-overexpressing Hep3B cell line. An in vivo intrahepatic injection study showed localization of MPs on the hepatic vessels and hepatic lobes up to 24 h after the injection without any shunting to the lung. Moreover, MPs efficiently inhibited tumor growth of Hep3B hepatic tumor xenografted mouse models. We expect that PLGA/pSMA-peptide-DOX MPs can be utilized as an effective intrahepatic drug delivery system for the treatment of HCC.

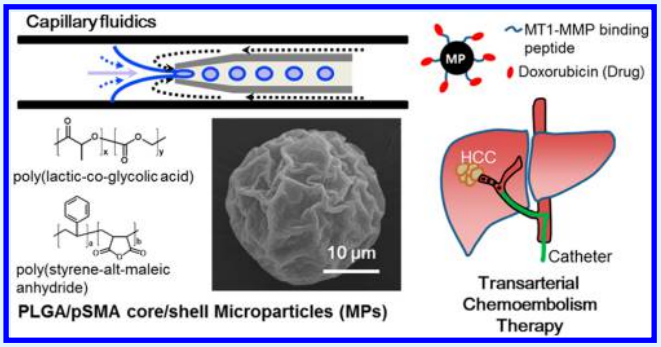

KEYWORDS: *microparticle, poly(D,L-lactide-co-glycolide), poly(styrene-alt-maleic anhydride), doxorubicin, hepatoma*

1. INTRODUCTION

Hepatocellular carcinoma (HCC) is a hypervascular tumor mainly caused by chronic liver infections, such as HBV (Hepatitis B virus), HCV (Hepatitis C virus), or cirrhosis.[1] HCC is one of the five leading causes of cancer death in the world, but its molecular nature is still poorly understood, and its treatment methods are limited. Currently, surgical resection and liver transplantation are the best curative methods for HCC, but patients still suffer from recurrence and metastasis after treatment.[2] To improve these surgical limitations, intrahepatic injections of chemotherapy drugs such as trans-catheter arterial chemoembolization (TACE) therapy have been considered as an alternative HCC treatment.[3] TACE is a combination therapy of arterial obstruction and local chemo-therapy that directly injects drugs into the lesions through a guided catheter. TACE therapy is needed to improve on currently used clinical drugs, and many researchers are interested in the development of novel biocompatible materials for application to TACE.

A particular drug delivery system is required for the intrahepatic delivery of cancer drugs. In this study, a capillary-focused microfluidic system was applied to create conjugated PLGA/pSMA core/shell microparticles with a 20 μm mean diameter. The microfluidic technique is now a well-established method for generating polymeric microparticles by homogeneous emulsion droplets. In addition, the particle size produced by microfluidics can be easily controlled depending on the flow rates of liquids in microchannels (<1000 um).[4,5] This technology offers low-cost and easy-to-use platforms for controlling fluid flow.[6] Hui Xie et al. developed a microfluidic system with dual inlet channels to produce the Janus particles of PLGA-encapsulated hydrophobic paclitaxel on one side and hydrophilic DOX on other side, demonstrating an encapsulation efficiency over 80%.[7]

Received: July 21, 2016
Accepted: December 14, 2016
Published: December 14, 2016

DOI: 10.1021/acsami.6b08994
ACS Appl. Mater. Interfaces 2017, 9, 71−79

Hydrophobic poly(lactic-*co*-glycolic acid) (PLGA) is a biocompatible and attractive polymer for biological and biomedical applications and has been approved by the FDA (Food and Drug Administration). Another polymer, amphiphilic poly(styrene-*alt*-maleic anhydride) (pSMA), is a commercial copolymer that includes reactive anhydride groups. These anhydride groups of pSMA can be easily conjugated with other amino, hydroxyl, or sulfhydryl groups.[8] Henry et al. developed a pH-responsive pSMA-allylamide derivative by reacting maleic anhydride groups of pSMA with primary alkylamines to obtain alkylamide derivatives capable of membrane disruption at endosomal pHs.[9] pSMA was also used clinically for delivery of the antitumor protein neocarzinostatin.[10] Michael P. Barannello et al. synthesized micelles of pSMA-*b*-PS (PS: polystyrene) for DOX loading and showed a stronger interaction between the drug and micelle core compared to other drugs, as shown through sustained release over 1 week.[11] Therefore, the pSMA polymer can be utilized for the conjugation of DOX with a peptide-linking capturing material in a PLGA-based drug delivery system.

Membrane-type 1 matrix metalloproteinase (MT1-MMP) is well-known transmembrane matrix metalloproteinase that maintains homeostasis of the extracellular matrix for tissue remodeling and development.[12,13] MT1-MMP is involved in the progression of different malignancies and is overexpressed on many cancer cells, especially hepatocellular carcinoma (HCC) with venous invasion.[14] MT1-MMP is also known to have versatile enzymatic proteolytic activity that degrades a specific peptide sequence (GPLPLRSWGLK).[15] Due to the overexpression of MT1-MMP on malignant cancer tissues, MT1-MMP and its peptide substrates have been utilized in various ways for cancer-specific targeted therapy and diagnosis.[16,17]

In this study, we present PLGA/pSMA core−shell structured MPs (microparticles) created with a microfluidic technique. After optimization of particle size by controlling the flow rates in the microchannel, the anticancer drug DOX and MT1-MMP-specific peptide were conjugated to the synthesized PLGA/pSMA MPs as a potential TACE material for HCC therapy. We have investigated their antitumor effects through in vitro and in vivo studies.

2. MATERIALS AND METHODS

2.1. Materials. Doxorubicin hydrochloride (M_w = 579.98), poly(styrene-*co*-maleic anhydride) (pSMA, styrene to maleic ratio 1.3:1, Mw = 1.6 kDa), dichloromethane (DCM, ≥ 99.5%), poly(vinyl alcohol) (PVA, M_w = 30−70 kDa, 87−90% hydrolyzed), *N*-ethyl-*N*′-(3-(dimethylamino)propyl) carbodiimide hydrochloride (EDC), and *N*-hydroxysuccinimide sodium salt (NHS) were purchased from Sigma-Aldrich. Poly(D,L-lactide-*co*-glycolide) (lactide to glycolic ratio 50:50, M_w = 30 kDa, Resomer RG 503H) was purchased from Boehringer-Ingelheim, Germany. Acetonitrile (ACN) and all other reagents were obtained from Daejung Korea Ltd. (Seoul, Korea). MT1-MMP-responsive peptide (GPLPLRSWGLK, M_w = 1223) was designed as described previously[15] and was purchased from GL Biochem (Seoul, Korea). Glass microcapillary tubes were purchased from VWR International, Korea. pSMA was purified before application as follows: Poly(styrene maleic anhydride) (1g) was reprecipitated with tetrahydrofuran (10 mL) in hexane (20 mL), washed with hexane to remove olefin impurities, and annealed at 120 °C for 20 h.[18]

2.2. Preparation of PLGA-Core/pSMA-Shell MPs Using a Microfluidic Technique. PLGA/pSMA microparticles were prepared using a capillary-focused microfluidic device, which was prepared as described previously.[19−21] (see Supporting Information S1). The schematic illustration of the microfluidic device is shown in Figure 1a.

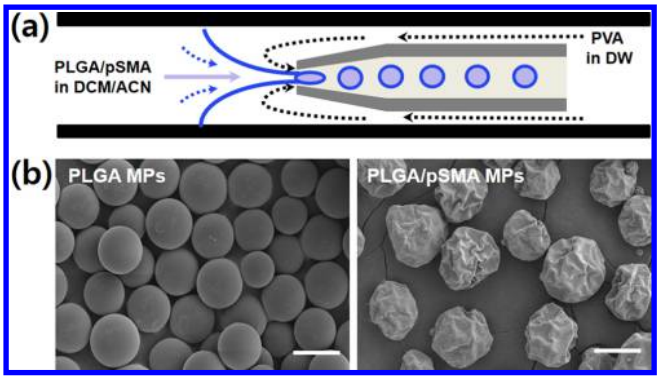

Figure 1. Microfluidic device system, (a) and SEM images of synthesized MPs (microparticles) (b); (a) PLGA (poly(lactic-*co*-glycolic acid))- and PLGA/pSMA (poly(lactic-*co*-glycolic acid)-grafted poly(lactic-*co*-glycolic acid)) MPs produced by dropwise addition of polymers in hydrophobic DCM/ACN (dichloromethane/acetonitrile) into water-soluble PVA (poly(vinyl alcohol)) in a continuous flow system. (b) Left: PLGA MPs, Right: PLGA/pSMA core−shell structured MPs. Scale bar =20 μm.

The internal oil phase (discontinuous phase) consisting of PLGA was dissolved in DCM (1.8% w/v) to form the core of the particles, whereas pSMA was dissolved in ACN (0.06% w/v) as a dispersed phase to form the shell of the particles. The PLGA and pSMA weight ratio was 10:1, and the volume ratio was 1:3. The outer aqueous phase (continuous phase) consisted of PVA (2% w/v) to stabilize the o/w emulsion. Both phases were flowed through the capillary using a syringe pump injector (LSP01−1A, Baoding Longer Precision Pumps). The syringe pump flow rates of the discontinuous and continuous phases were 0.035 and 1 mL/min, respectively. The droplets were physically formed at the beginning of the capillary tip. The resulting PLGA/pSMA microparticle products were charged into a beaker that was heated at 35 °C with gentle stirring overnight at 300 rpm to evaporate the solvent. Then, microparticles were purified by centrifugation (Centrifuge 5415R, Eppendorf AG Hamburg, Germany) at 3600 rpm for 5 min and washed with distilled water to eliminate the excess solvent and surfactant (5 time). The microparticles were stored at 4 °C for further studies.

2.3. Chemical Conjugation of PLGA/pSMA MPs with Peptide and DOX. The DOX-conjugated PLGA/pSMA MPs were prepared with an EDC/NHS system. First, 100 mg of PLGA/pSMA MPs were added into 10 mL of borated buffer (50 mM pH 8.5) to form the dicarboxylate groups by hydrolysis of the maleic anhydride groups of pSMA. Next, 1 mg of EDC and 1.2 mg of NHS were introduced to activate those carboxylate groups so that they could react with the primary amino groups of peptides and DOX (Figure 2). Then, MT1-MMP-responsive peptide (7 mg) or DOX (3.2 mg) was charged into the mixture and stirred at 300 rpm overnight at room temperature. The obtained products were centrifuged at 3600 rpm for 5 min and redispersed in distilled water. Five cycles of centrifugation were performed to remove unreacted components. Then, peptide-conjugated PLGA/pSMA MPs, 3.2 mg DOX, 1 mg EDC, and 1.2 mg NHS were mixed into 10 mL of phosphate buffer and stirred overnight at 300 rpm at room temperature. The resulting PLGA/pSMA-peptide-DOX MPs were collected after centrifugation at 3600 rpm for 5 min. The samples were then redispersed in distilled water and centrifuged 5 times to eliminate unreacted DOX.

2.4. Physical Characterizations of MPs. The mean particle size and morphology of the microparticles were examined by scanning electron microscopy (SEM) (Hitachi S-4800, Japan). The MPs were dispersed in distilled water, and the dispersions were dropped onto a cover glass and dried in a vacuum chamber for 24 h. The dried samples were attached to an aluminum stub and coated with platinum. The coated samples were then observed at 5 kV.

The functional group of samples before and after modification of amine on pSMA was analyzed by Fourier transform infrared (FTIR)

DOI: 10.1021/acsami.6b08994
ACS Appl. Mater. Interfaces 2017, 9, 71−79

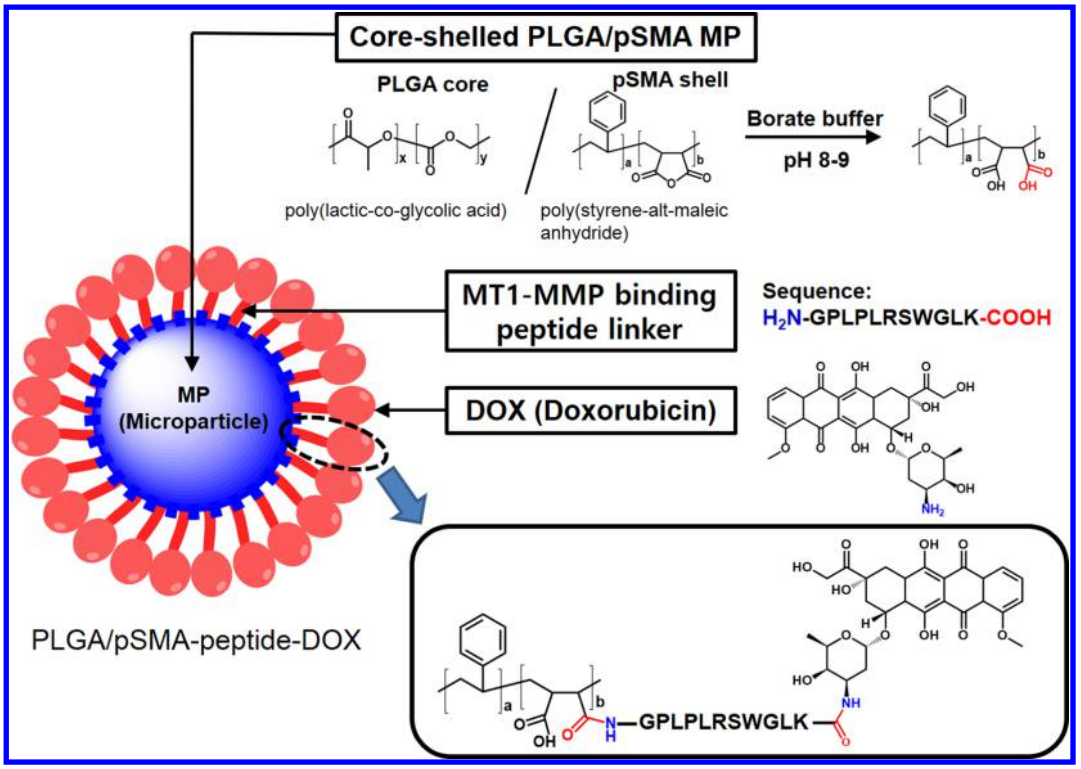

Figure 2. Synthetic scheme of MT1-MMP (membrane type matrix metalloproteinase 1)-targeting peptide introduced into DOX (doxorubicin)-conjugated PLGA/pSMA MPs.

spectroscopy (VERTEX 80 V) and X-ray photoelectron spectroscopy (XPS).

The DOX-conjugated MPs were examined by confocal laser scanning microscopy at an excitation wavelength of 480 nm and emission wavelength of 550 nm (CLSM, Carl Zeiss, LSM510, Gottingen, Germany).

2.5. Drug Release Study. The release of DOX from MPs was measured in phosphate buffered saline (PBS) with a pH of 7.4 or 5.4 with a fluorescence spectrometer over 28 days. Next, 20 mg of microparticles (0.5 mg of DOX) was dispersed in a conical tube with 50 mL of PBS and shaken continuously at 100 rpm for 37 °C. The tubes were centrifuged at specific time intervals, and 1 mL of the supernatant was collected for HPLC. This analysis was conducted on 3 samples of each MP.

2.6. In Vitro Cellular Uptake of DOX. The cells were seeded at 1 × 10^5 cells/well in DMEM medium and cultured in 12-well plates for 1 day. The DMEM was replaced with 25 nM of DOX in FBS-free fresh media for each formulation at 37 °C for 24 h. The MPs were removed, and the cells were washed three times with PBS. The cells were harvested by trypsinization and resuspended in distilled water. The cells were lysed by ultrasonication (Sonics webra cell) for 1 min and centrifuged at 13 200 rpm for 10 min. Finally, the cellular supernatant and cellular DOX uptake were measured at an excitation wavelength of 480 nm and emission wavelength of 550 nm (Nanoplate reader, Thermo, U.S.A.).

2.7. Cytotoxicity Test. Human hepatocellular carcinoma Hep3B cells were treated with DOX-coated PLGA MPs (with or without pSMA) at a concentration of 25 nM of DOX, and cellular toxicity was determined with a WST assay. The cells were seeded in 96-well plates at a density of 1 × 10^4 cells/well in DMEM medium. The medium was washed off and replaced with new media containing microparticles and free drug. After a 24 h incubation, cells were washed twice with cold PBS to eliminate the remaining drugs. Subsequently, the cells were treated with 100 μL media and 10 μL/well of WST (EZ-Cytox) and incubated for 30 min. The absorbance was measured at a wavelength of 450 nm using a microplate spectrophotometer (Bio Rad, xMark). Cytotoxicity was expressed as the percentage of the control. All experiments were performed in triplicate.

2.8. Intahepatic Portal Vein Injection of MPs. Male SD rats 6−7 weeks of age (300−350 g, Orient Bio Co., Korea) were selected for intrahepatic injection studies. All animal care and procedures were conducted according to the Guiding Principles in the use of animal establishment by Inha University. The rats were anesthetized via ethyl ether. The abdomen was opened, and 0.3 mL of the PLGA/pSMA-DOX MPs (5 mg/kg of DOX) in PBS were then injected into the portal vein. After injection of the MPs, the needle was kept in the portal vein for 5 min and slight pressure was applied using cotton soaked in ethanol. After 1 or 24 h, the liver and lung were carefully excised from the rats and washed several times with PBS solution. The samples were analyzed with a fluorescence imaging machine (FOBI, NeoScience Co., Suwon, Korea).

2.9. In Vivo Antitumor Activities of DOX-Coated MPs. Male Balb/c nude mice were purchased from Orient Bio Co (Seoul, Korea). Human tumor Hep3B cells (2 × 10^6 cells/mouse) were suspended in 100 μL PBS and inoculated into nude mice (7−8 weeks old) under anesthesia. Mice were grouped and monitored at least twice a week for evidence of tumor development and quantification of tumor size. The antitumor study was performed when tumor size reached approximately 100 mm^3. In the control groups, the mice were injected with free DOX (2 mg/kg) in PBS 4 times at 4-day intervals via the tail vein. In the treatment groups, PLGA/pSMA-DOX and PLGA/pSMA-peptide-DOX MPs (DOX equivalent to 5 mg/kg) were intratumorally injected only one time. The tumor size and body weight of each mouse were monitored three times a week for 28 days. Tumor size was determined by vernier caliper measurements, and tumor volume was calculated as [length × (width × width)/2].

For H&E and TUNEL staining, the tumor was fixed with 4% paraformaldehyde overnight and embedded in paraffin. The specimen was sectioned to a thickness of 3 μm and stained using hematoxylin and eosin (H&E). TUNEL staining was prepared using a TUNEL kit according to the manufacturer's protocol.

2.10. Statistical Analysis. All data were expressed as the mean ± the standard error of the mean of three independent experiments.

DOI: 10.1021/acsami.6b08994
ACS Appl. Mater. Interfaces 2017, 9, 71−79

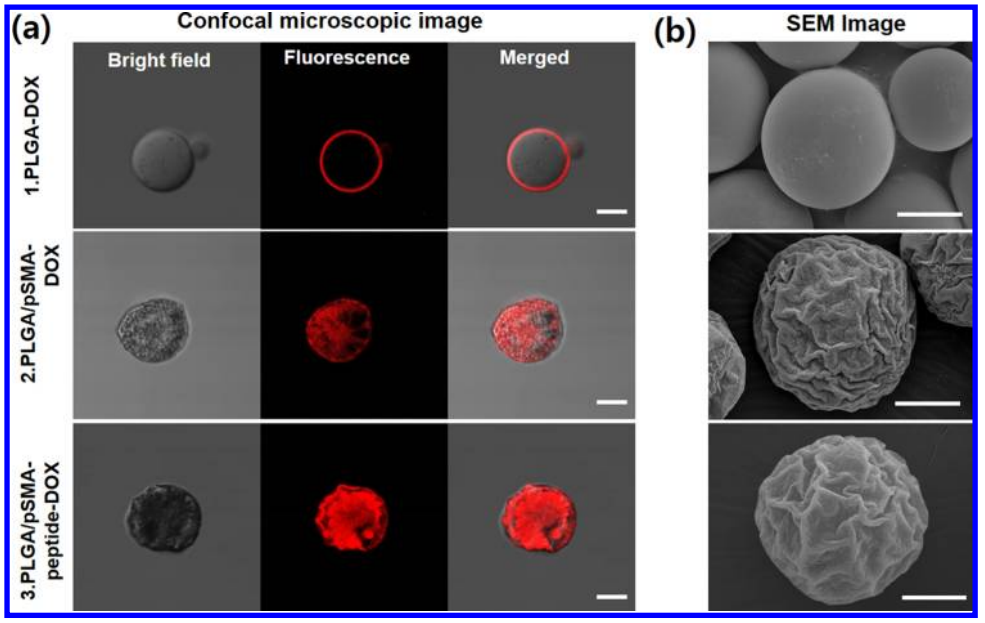

Figure 3. Confocal microscopic (a) and SEM (b) images of DOX-conjugated MPs: (1) PLGA-DOX MPs, (2) PLGA/pSMA-DOX MPs, and (3) PLGA/pSMA-peptide-DOX MPs. Red on the confocal microscopic images indicates DOX fluorescence. Scale bar =10 μm.

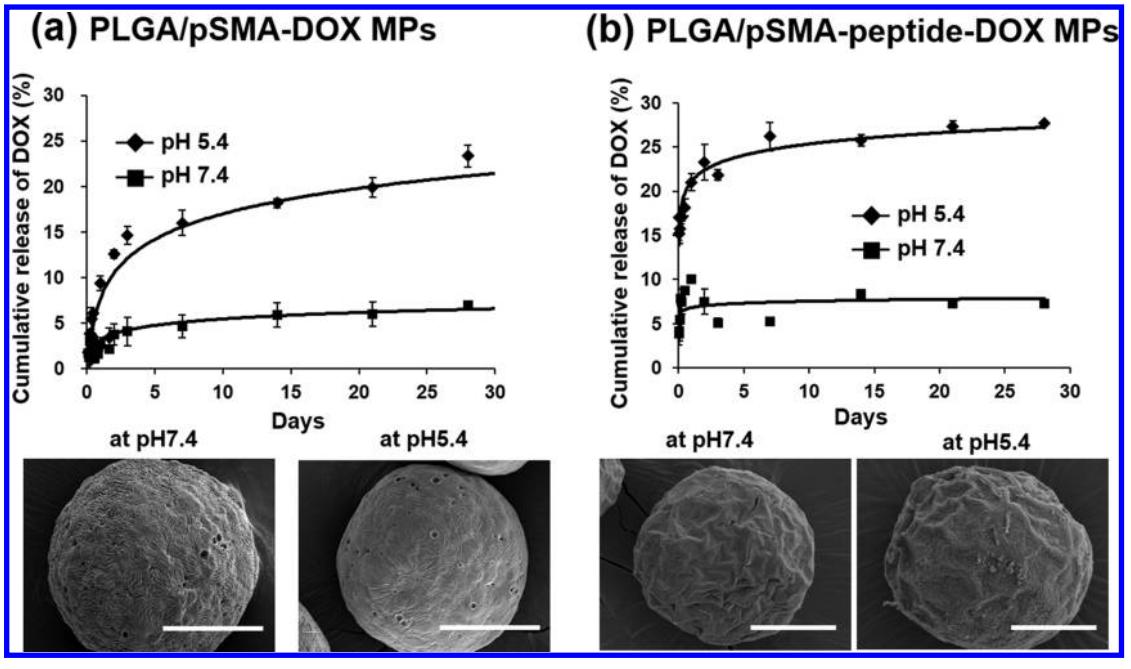

Figure 4. In vitro drug release at pH 5.4 (♦) and 7.4 (■) for 28 days: PLGA/pSMA-DOX MPs (a) and PLGA/pSMA-peptide-DOX MPs (b) with the same concentration of DOX (20 μg/mL). (Up) Cumulative release profiles of DOX from MPs depending on time. (Down) SEM images of MPs at different pH conditions (scale bar =10 μm).

Intergroup comparison of data was analyzed with a Student's *t* test at a significance level of α = 0.05.

3. RESULTS AND DISCUSSION

3.1. Synthesis and Characterization of PLGA/pSMA Core/Shell MPs. For development of the core/shell structured drug delivery carrier microparticles (MPs), we used poly D,L-lactic-*co*-glycolic acid (PLGA) as a hydrophobic polymer to form a core particle and amphiphilic poly(styrene maleic anhydride) (pSMA) to encapsulate the PLGA surface. Using a microfluidic technique, the PLGA and pSMA mixture in hydrophobic dichloromethane (DCM)/acetonitrile (ACN) cosolvent was added dropwise into the continuous flow of aqueous PVA solution (Figure 1(a)). To control MP size, the flow rate of PLGA/pSMA in the dispersed phase was varied from 10 to 50 μL/min under a constant flow (1000 μL/min) of aqueous PVA. We confirmed that the particle sizes of MPs increased from 12 to 43 μm as the flow rate increased in the dispersed phase (experimental process was included in SI S1 and the size distribution is shown in Table S1). Figure 1(b) shows the SEM images of synthesized PLGA MPs and PLGA/pSMA MPs obtained from the 10 μL/min flow condition in the dispersed phase. The PLGA particles (Figure 1(b) left) showed smooth surfaces and were approximately 19 ± 2 μm in

DOI: 10.1021/acsami.6b08994
ACS Appl. Mater. Interfaces 2017, 9, 71−79

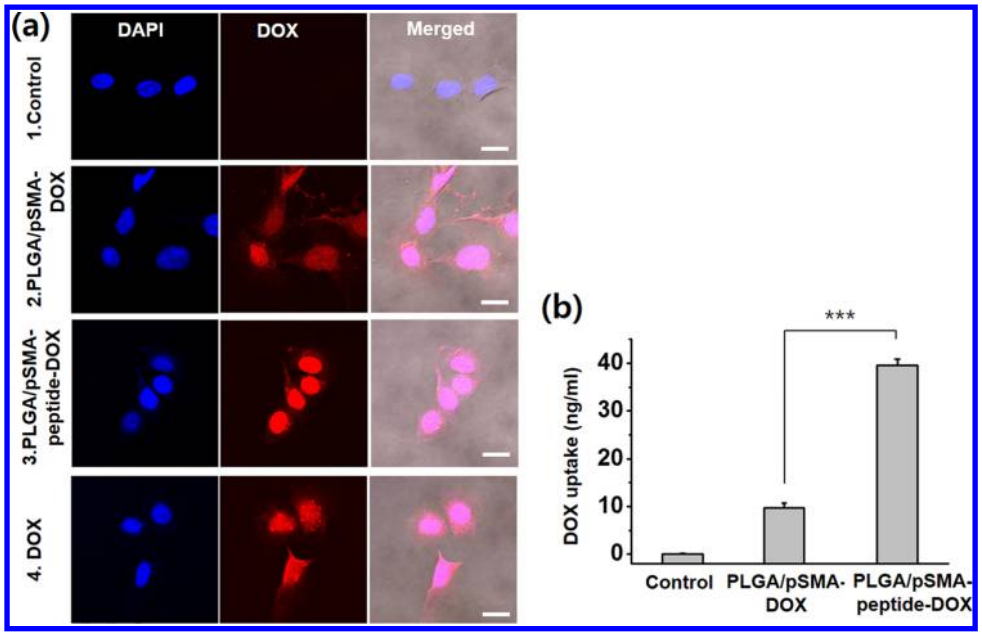

Figure 5. Fluorescence images (a) and intracellular contents of DOX (b) in the Hep3B cell line: (1) Control (no treatment), (2) PLGA/pSMA-DOX MPs, (3) PLGA/pSMA-peptide-DOX MPs, and (4) free DOX (25 nM) treatment. Cells were treated with MPs with the same concentration of DOX (25 nM) and incubated for 24 h. (a) For cellular imaging, all cells were further treated with DAPI, and fluorescence images passing through the 450 nm (DAPI) and 550 nm (DOX) emission filters were obtained with a LSM510 confocal microscope. Scale bar =20 μm. (b) To confirm the intracellular content of DOX, cells were lysed, and the concentration of DOX was determined by interpolation with a calibration curve of the parent drug using a fluorescence spectrometer at 560 nm.

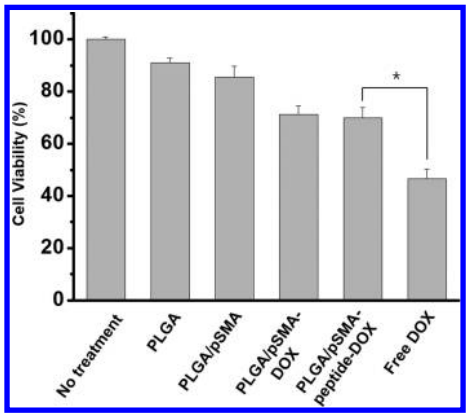

Figure 6. Cytotoxicity of MPs: Hep3B cells were incubated with MPs (14.5 μg/mL, DOX = 25 nM) and free DOX (25 nM) for 24 h, and a cell viability test was performed using a WST assay as described in the manufacturer's protocol.

diameter. Interestingly, when the surface of the PLGA particles was coated with pSMA (Figure 1(b) right), the whole particle morphology became irregular with a rough surface, and the particle size increased to 22 ± 3 μm. We hypothesized that hydrophilic pSMA diffused from the hydrophobic PLGA core to form an outer shell during droplet formation.[22]

For further confirmation of core/shell structured MPs, we further performed FT-IR analysis (see the Figure S1(a)). PLGA MPs showed the characteristic absorption peaks of the polymer backbone at 3000−2700 cm^{-1} (C—H stretching), 1900−1550 cm^{-1} (C═O stretching), and 1800−1150 cm^{-1} (C—O stretching). In the case of pSMA-free polymer, the peak at 720−680 cm^{-1} was assigned to C—H stretching of monosubstituted benzene ring from the styrene moiety of the polymer backbone. This peak was also visible in the spectrum of the PLGA/PSMA core/shell MP sample.

3.2. Conjugation of Doxorubicin (DOX) to PLGA/pSMA MPs. To stably load DOX onto the PLGA/pSMA MPs and utilize MT1-MMP-responsive drug release properties, we conjugated DOX to the PLGA/pSMA MPs with MT1-MMP-overexpressed tumor-targeting peptide as a spacer.

Figure 2 shows the schematic illustration of PLGA/pSMA-peptide-DOX MPs. Succinic anhydride moieties obtained from styrene-maleic anhydride copolymerization of the surface pSMA from the PLGA/pSMA MPs were hydrolyzed and changed to carboxyl groups under physiological buffer conditions. Then, the N-terminal group of the peptide was reacted with MPs in the presence of EDC/NHS and PLGA/pSMA MP-peptide conjugates, which were formed by amide bonding. The opposite site of the peptide, the C-terminal group, was subsequently conjugated with the amine moiety of DOX using the same method. As a control experiment, we also prepared PLGA/pSMA-DOX MPs without the peptide linker and evaluated their drug release properties through in vitro and in vivo tests.

DOX and MT1-MMP peptide conjugations to PLGA/pSMA MPs were confirmed by FT-IR analysis (see Figure S1(b)). The characteristic 1580 cm^{-1} peak of PLGA/pSMA-DOX MPs and PLGA/pSMA-peptide-DOX MPs was clearly shown in the spectrum (dashed line) due to the N—H bending and C—N stretching of amide bonds and is compared with a control PLGA/pSMA MPs. The existence of DOX on the MPs was also confirmed by XPS analysis (see Figure S2). PLGA/pSMA MPs showed only a C 1s (carbon 1s, 284.8 eV) peak and an O 1s (oxygen 1s, 530.1 eV) peak, but the P PLGA/pSMA-DOX MPs showed an additional peak at 400.8 eV (N 1s), from the nitrogen components of DOX.

To visualize DOX-conjugated MPs, we further performed confocal microscopic and scanning electron microscopic image analysis (Figure 3). As shown in the confocal microscopic images in Figure 3(a), PLGA MPs (1) that reacted with DOX

DOI: 10.1021/acsami.6b08994
ACS Appl. Mater. Interfaces 2017, 9, 71−79

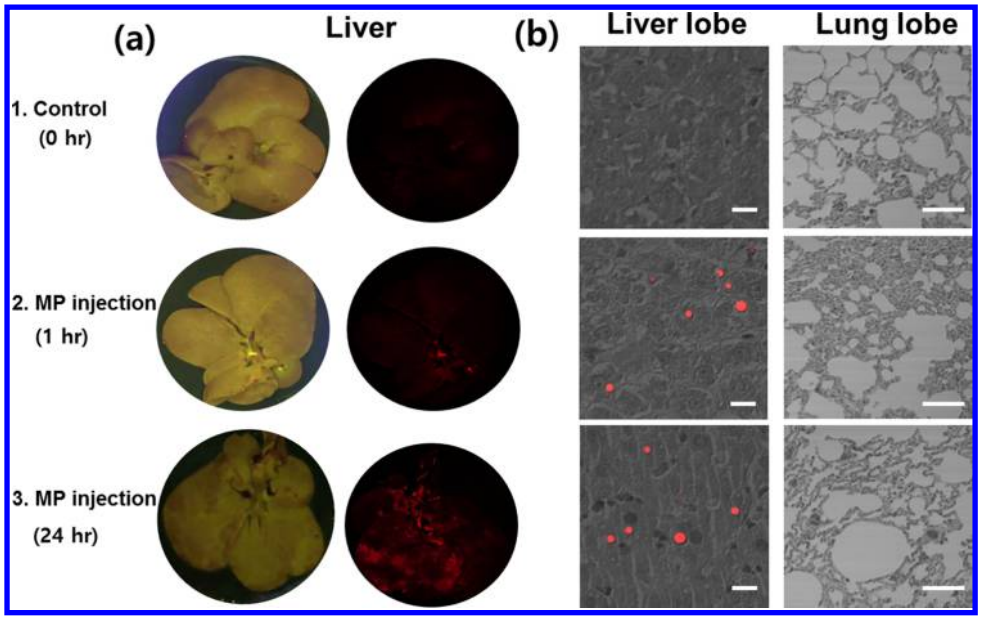

Figure 7. Photographic images of liver (a) and microscopic images of liver and lung lobe (b) extracted from rats: (1) without MPs and with MPs (4.6 g/kg, DOX conc.= 5 mg/kg) for 1 h (2) and 24 h (3). (a) Left: photographs of livers, right: fluorescence images, (b) confocal microscopic image of a liver lobe (left) and a lung lobe (right) as a control. Red color indicates DOX fluorescence. Scale bar =50 μm.

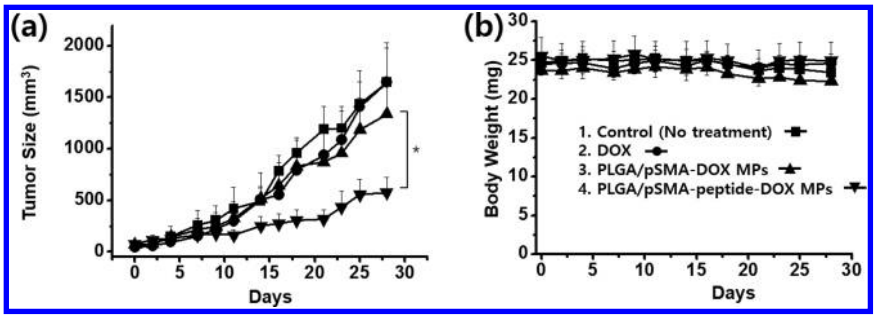

Figure 8. Tumor growth inhibition of human tumor cell line Hep3B xenografts in male Balb/c nude mice: (a) Tumor growth vs time, and (b) body weight of each mouse on each day. Sample: (1) control (■), (2) free DOX (2 mg/kg × 4 times every 4 days, I.V) (●), (3) PLGA/pSMADOX MPs (5 mg/kg × 1 time I.T) (▲), and (4) PLGA/pSMA-peptide-DOX MPs (5 mg/kg × 1 time I.T)(▼).

in the presence of EDC/NHS showed weak fluorescence of DOX on the MP surface. However, PLGA PLGA/pSMA-DOX MPs (2) and PLGA/pSMA-peptide-DOX MPs (3) showed strong red fluorescence because large amount of DOX were conjugated onto their surfaces. The SEM images in Figure 3 (b) show that there were no morphological changes of MPs after DOX or peptide-DOX conjugation.

DOX loading efficiency of each sample was calculated as described in SI S4. We prepared three independent sample sets and found loading efficiencies of 2.9 ± 0.26% (PLGA/pSMA-DOX MPs) and 2.6 ± 0.14% (PLGA/pSMA-peptide-DOX MPs), with encapsulation efficiencies of 88.7 ± 8.1% and 91.1 ± 5.7%, respectively.

3.3. pH-Dependent DOX Release from MPs. Synthesized PLGA/pSMA-DOX and PLGA/pSMA-peptide-DOX MPs were exposed to PBS buffer under physiological (pH 7.4) and acidic (p H 5.4) conditions to measure the release of DOX and confirm the potential applications of DOX-loaded MPs for HCC therapy. As shown in Figure 4, the DOX release rate and amount were strongly dependent on pH. PLGA/pSMA-DOX (Figure 4(a)) and PLGA/pSMA-peptide-DOX MPs (Figure 4(b)) showed faster release of DOX in an acidic buffer (pH 5.4) than at a neutral (pH 7.4) condition. After 28 h, cumulative DOX release from PLGA/pSMA-DOX MPs and PLGA/pSMA-peptide-DOX MPs was approximately ~23% and ~28% at pH 5.4 and ~7% and ~8% at pH 7.4, respectively. We conjugated the DOX molecules with ring-opened maleic anhydride groups of the outer pSMA shell of MPs by amide bonding, but maleic anhydride can be cleaved when the carboxyl groups are protonated in an acidic environment.[23,24] Moreover, pH value in the extracellular environment of a tumor is more acidic than that of normal tissue due to the high glycolysis and lactic acid production.[25,26] The acidic environment near the tumor may trigger the rapid release of DOX from the MPs, causing efficient tumor targeting and enhanced cellular toxicity. This may be particularly true in the case of PLGA/pSMA-peptide-DOX MPs due to their peptide sequences with MT1-MMP specificity. The morphologies of MPs under different pH conditions (pH 7.4 and 5.4) were also confirmed using SEM image analysis. As shown in Figure 4 (bottom), the PLGA/pSMA-DOX MPs and PLGA/pSMA-peptide-DOX MPs had rougher surfaces under physiological buffer conditions (pH 7.4) than they did at pH 5.4. These results indicate that the surface pSMA polymers on MPs change their inherent physical and chemical properties depending on pH.

DOI: 10.1021/acsami.6b08994
ACS Appl. Mater. Interfaces 2017, 9, 71−79

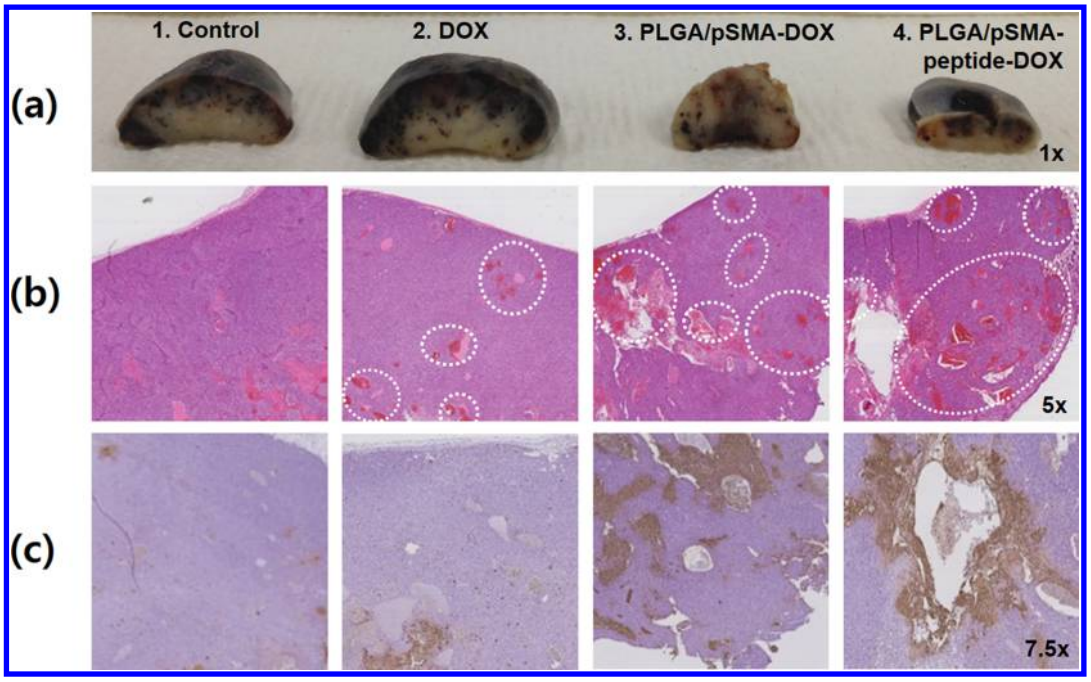

Figure 9. Hep3B tumor images. (a) cross sectional images of each tumor after H&E (5x, b) and TUNEL staining (7.5x, c); (1) no treatment, (2) free DOX (2 mg/kg), (3) PLGA/pSMA-DOX (1.8 g/kg, DOX conc.= 2 mg/kg), and (4) PLGA/pSMA-peptide-DOX (1.8 g/kg, DOX conc.= 2 mg/kg). In H&E staining images (b), dashed circles indicate apoptotic or necrotic cell death. For TUNEL staining images (c), the brown color represents apoptosis-predominant regions.

3.4. Cellular Drug Uptake. On the basis of the pH-dependent DOX release from MPs, we further investigated the cellular entry of DOX in a human hepatoma Hep3B cell line that overexpresses MT1-MMP (Expression level of MT1-MMP was confirmed by RT-PCR, and its analytical data were shown in SI S5 and Figure S3). DOX is a well-known chemotherapeutic drug that can intercalate between DNA base pairs, resulting in inhibition of transcription and DNA synthesis.[27] To confirm cellular entry and nuclear accumulation of DOX released from MPs, we treated the Hep3B cells with DOX-conjugated MPs and incubated for 24 h. After removal of MPs, cells were fixed with 4% paraformaldehyde and further treated with DAPI for nuclear staining. Figure 5(a) shows confocal microscopic imaging of Hep3B cells. DOX fluorescence (red) in PLGA/pSMA-DOX MP-(2), PLGA/pSMA-peptide-DOX MP-(3), and free DOX-(4) treated cells colocalized with DAPI in the nucleus. To confirm intracellular DOX contents, cells were further lysed and resuspended, and DOX was analyzed with a fluorescence quantification method. As shown in Figure 5(b), the cellular uptake of DOX released from PLGA/pSMA-DOX MPs was ~10 ng/mL, and that of PLGA/pSMA-peptide-DOX MPs was ~40 ng/mL. These results suggest that the peptide-linked DOX was more efficiently released because the membrane MT1-MMP overexpressed in Hep3B cells induces its targeting peptide sequence degradation.[28,29]

3.5. Cytotoxicity of MPs. The cytotoxicity testing of DOX was carried out using a WST assay. Figure 6 shows the cell viability percentage of Hep3B cells after a 24 h incubation with MPs. The concentration of MPs was 0.5 μg/mL, and DOX- and peptide/DOX-conjugated MPs included the same concentration of DOX (25 nM). Previous results have shown that PLGA polymers composed of lactic and glycolic acid units are nontoxic and have excellent biocompatibility.[30] However, in our case, PLGA MPs showed ~90% viability, and the viability of PLGA/pSMA samples was slightly lower than that of neat PLGA because of the toxicity of pSMA itself. PLGA/pSMA-DOX MP- and PLGA/pSMA-peptide-DOX MP-treated cells showed around ~70% viability after 24 h. This suggests that DOX was released from the MP surfaces and affected cellular toxicity during the incubation. As a negative control, free DOX presented the highest toxicity (~50%) in Hep3B cells.

3.6. Intrahepatic Distribution and Antitumor Effect of MPs. An intrahepatic injection study was performed to evaluate the PLGA/pSMA-DOX MPs as a potential therapeutic reagent for HCC. MPs were injected directing into the portal vein of Sprague−Dawley rats (male, 250−300 g) after opening the abdomen. After 1 or 24 h incubation with PLGA/pSMA-DOX MPs, the liver and lung tissues were extracted from the rats and analyzed for fluorescence. As shown in Figure 7(a), the control liver (without MPs, Figure 7(a), 1) did not show any fluorescence, but the sample incubated with MPs for 1 h (Figure 7(a), 2) showed central localization in the liver, shown as red spots. After a 24 incubation with MPs (Figure 7(a), 3), the rats showed diffuse fluorescence in all of the liver, and the fluorescence intensity increased due to the continuous inflow of MPs into the liver from the portal vein. In Figure 7 (b), confocal microscopic images show the specific accumulation of MPs in the liver tissue. In the liver lobe images (Figure 7(b) left), red fluorescent MPs (Figure 7(b), 2 and 3) were clearly shown in all cases except the control (Figure 7(b), 1), and there was no red fluorescence in the lung lobe images (Figure 7(b) right). These results indicate that the PLGA/pSMA-DOX MPs circulating through the blood vessels can reach terminal liver tissues without nonspecific invasion into other organs. Size control of the MPs is very important for localization on the hepatic tumor vessels; we suggest that the ~20-μm-sized MPs used in this study showed efficient passive diffusion, so this particle size may be suitable for potential embolization therapy in HCC.

DOI: 10.1021/acsami.6b08994
ACS Appl. Mater. Interfaces 2017, 9, 71−79

In vivo antitumor effects of MPs were also studied to determine whether PLGA/pSMA-peptide-DOX treatment leads to controlled drug release and tumor regression in a human hepatocellular carcinoma Hep3B xenografted Balb/C nude mouse model. For this study, Hep3B cells subcutaneously injected into the back of each mouse were maintained for 2 weeks. After confirmation of appropriate tumor size, MPs were injected intratumorally, and antitumor activity was monitored over 28 days. As shown in Figure 8(a), control tumor volumes of mice without drug treatment reached ~1800 mm^3 (approximately 15 times more than the initial volume (120 mm^3)) after 28 days, and the free DOX treatment did not show any remarkable tumor suppression effects compared with the control. Treatment with PLGA/pSMA-DOX MPs slightly slowed tumor growth, and this group's tumor volumes reached ~1300 mm^3 (approximately 10 times more than the initial volume) after 28 days. Interestingly, the tumors of PLGA/pSMA-peptide-DOX MP-treated mice were significantly reduced compared with the control, resulting in volumes of ~570 mm^3 (~5 times the starting volume) during the same time interval. These results suggest that the MT1-MMP-targeting peptide sequence linker between MPs and DOX in PLGA/pSMA-peptide-DOX MPs enhances DOX release in the MT1-MMP-predominant condition and the self-released DOX from the biodegradable PLGA and pSMA polymer composite. Figure 8(b) shows the body weight profiles of mice over time. As shown in the data, all mice maintained a steady body weight (~25 mg). This indicates that there was no serious toxicological effect due to the appropriate dosage of drugs in these mice.

Then, the tumors were excised from mice (Figure 9(a) shows an extracted tumor), and histological staining was performed with H&E and TUNEL staining. In Figure 9(b), H&E staining images show that the PLGA/pSMA-DOX MP- and PLGA/pSMA-peptide-DOX MP-treated samples showed increased apoptotic and necrotic cell death in the tumor microenvironment. The TUNEL staining (Figure 9(c)) images also showed increased apoptosis in the MP-treated samples.

4. CONCLUSIONS

In this paper, we successfully produced size-controlled PLGA/pSMA core−shell MPs using a microfluidic technique. Synthesized MPs were conjugated with DOX, and the MT1-MMP-targeting peptide was introduced as a linker molecule between DOX and MPs to enhance tumor targeting. These MPs showed pH-sensitive sustained drug release for one month. Moreover, in vitro and in vivo release studies of MPs demonstrated that DOX released from PLGA/pSMA-peptide-DOX MPs has more efficient cellular entry into Hep3B cells and improved tumor suppression compared to PLGA/pSMA-DOX MPs. These results suggest that this material can be deployable as a potential candidate for TACE therapy for HCC.

■ ASSOCIATED CONTENT

Supporting Information

The Supporting Information is available free of charge on the ACS Publications website at DOI: 10.1021/acsami.6b08994.

Preparation of capillary-focused microfluidics, FT-IR analysis, XPS analysis, loading/encapsulation efficiency of DOX to MPs and RT-PCR study (PDF)

■ AUTHOR INFORMATION

Corresponding Author

*Tel: +82-32-890-1183. Fax: +82-32-890-1199. E-mail: Sugeun.Yang@inha.ac.kr (S.-G.Y.).

Author Contributions

#These authors contributed equally.

Notes

The authors declare no competing financial interest.

■ ACKNOWLEDGMENTS

This work was supported by the Basic Science Research Program through the National Research Foundation of Korea, (NRF) funded by the Ministry of Science, ICT, and Future Planning (2014R1A2A2A04006562) and partially supported by World Class Smart Laboratory(WCSL) Program of Inha University, Korea.

■ REFERENCES

(1) Wong, I. N.; Leung, T.; Ho, S.; Lau, W. Y.; Chan, M.; Johnson, P. J. Semiquantification of Circulating Hepatocellular Carcinoma Cells by Reverse Transcriptase Polymerase Chain Reaction. *Br. J. Cancer* **1997**, *76* (5), 628−633.

(2) Blum, H. E. Hepatocellular Carcinoma: Therapy and Prevention. *World J. Gastroenterol.* **2005**, *11* (47), 7391−7400.

(3) Lewandowski, R. J.; Geschwind, J. F.; Liapi, E.; Salem, R. Transcatheter Intraarterial Therapies: Rationale and Overview. *Radiology* **2011**, *259* (3), 641−657.

(4) Nunes, J. K.; Tsai, S. S. H.; Wan, J.; Stone, H. A. Dripping and Jetting in Microfluidic Multiphase Flows Applied to Particle and Fibre Synthesis. *J. Phys. D-Appl. Phys.* **2013**, *46* (11), 1−20.

(5) Sah, E.; Sah, H. Recent Trends in Preparation of Poly(lactide-co-glycolide) Nanoparticles by Mixing Polymeric Organic Solution with Antisolvent. *J. Nanomater.* **2015**, *2015*, 1−22.

(6) Xu, Q.; Hashimoto, M.; Dang, T. T.; Hoare, T.; Kohane, D. S.; Whitesides, G. M.; Langer, R.; Anderson, D. G. Preparation of Monodisperse Biodegradable Polymer Microparticles Using a Microfluidic Flow-Focusing Device for Controlled Drug Delivery. *Small* **2009**, *5* (13), 1575−1581.

(7) Xie, H.; She, Z.-G.; Wang, S.; Sharma, G.; Smith, J. W. One-Step Fabrication of Polymeric Janus Nanoparticles for Drug Delivery. *Langmuir* **2012**, *28* (9), 4459−4463.

(8) Khazaei, A.; Saednia, S.; Saien, J.; Kazem-Rostami, M.; Sadeghpour, M.; Borazjani, M. K.; Abbasi, F. Grafting Amino Drugs to Poly(styrene-alt-maleic Anhydride) as a Potential Method for Drug Release. *J. Braz. Chem. Soc.* **2013**, *24* (7), 1109−1115.

(9) Henry, S. M.; El-Sayed, M. E. H.; Pirie, C. M.; Hoffman, A. S.; Stayton, P. S. pH-Responsive Poly(styrene-alt-maleic anhydride) Alkylamide Copolymers for Intracellular Drug Delivery. *Biomacromolecules* **2006**, *7* (8), 2407−2414.

(10) Maeda, H.; Ueda, M.; Morinaga, T.; Matsumoto, T. Conjugation of Poly(styrene-co-maleic acid) Derivatives to the Antitumor Protein-Neocarzinostatin: Pronounced Improvements in Pharmacological Properties. *J. Med. Chem.* **1985**, *28*, 455−461.

(11) Baranello, M. P.; Bauer, L.; Benoit, D. S. W. Poly(styrene-alt-maleic anhydride)-Based Diblock Copolymer Micelles Exhibit Versatile Hydrophobic Drug Loading, Drug-Dependent Release, and Internalization by Multidrug Resistant Ovarian Cancer Cells. *Biomacromolecules* **2014**, *15* (7), 2629−2641.

(12) d'Ortho, M. P.; Will, H.; Atkinson, S.; Butler, G.; Messent, A.; Gavrilovic, J.; Smith, B.; Timpl, R.; Zardi, L.; Murphy, G. Membrane-type Matrix Metalloproteinases 1 and 2 Exhibit Broad-spectrum Proteolytic Capacities Comparable to Many Matrix Metalloproteinases. *Eur. J. Biochem.* **1997**, *250* (3), 751−757.

(13) Ohuchi, E.; Imai, K.; Fujii, Y.; Sato, H.; Seiki, M.; Okada, Y. Membrane Type 1 Matrix Metalloproteinase Digests Interstitial

DOI: 10.1021/acsami.6b08994
ACS Appl. Mater. Interfaces 2017, 9, 71−79

Collagens and Other Extracellular Matrix Macromolecules. *J. Biol. Chem.* **1997**, *272* (4), 2446−2451.
(14) Chen, X.; Cheung, S. T.; So, S.; Fan, S. T.; Barry, C.; Higgins, J.; Lai, K. M.; Ji, J. F.; Dudoit, S.; Ng, I. O. L.; van de Rijn, M.; Botstein, D.; Brown, P. O. Gene Expression Patterns in Human Liver Cancers. *Mol. Biol. Cell* **2002**, *13* (6), 1929−1939.
(15) Park, J.; Yang, J.; Lim, E.-K.; Kim, E.; Choi, J.; Ryu, J. K.; Kim, N. H.; Suh, J.-S.; Yook, J. I.; Huh, Y.-M.; Haam, S. Anchored Proteinase-Targetable Optomagnetic Nanoprobes for Molecular Imaging of Invasive Cancer Cells. *Angew. Chem., Int. Ed.* **2012**, *51* (4), 945−948.
(16) Zhu, L.; Wang, H. L.; Wang, L.; Wang, Y.; Jiang, K.; Li, C.; Ma, Q. J.; Gao, S.; Wang, L. P.; Li, W.; Cai, M. J.; Wang, H. D.; Niu, G.; Lee, S.; Yang, W.; Fang, X. X.; Chen, X. Y. High-affinity Peptide against MT1-MMP for In Vivo Tumor Imaging. *J. Controlled Release* **2011**, *150* (3), 248−255.
(17) Zhu, L.; Zhang, F.; Ma, Y.; Liu, G.; Kim, K.; Fang, X. X.; Lee, S.; Chen, X. Y. In Vivo Optical Imaging of Membrane-Type Matrix Metalloproteinase (MT-MMP) Activity. *Mol. Pharmaceutics* **2011**, *8* (6), 2331−2338.
(18) Pompe, T.; Zschoche, S.; Herold, N.; Salchert, K.; Gouzy, M. F.; Sperling, C.; Werner, C. Maleic anhydride copolymers - A Versatile Platform for Molecular Biosurface Engineering. *Biomacromolecules* **2003**, *4* (4), 1072−1079.
(19) Zhang, H.; Ju, X. J.; Xie, R.; Cheng, C. J.; Ren, P. W.; Chu, L. Y. A Microfluidic Approach to Fabricate Monodisperse Hollow or Porous Poly(HEMA-MMA) Microspheres using Single Emulsions as Templates. *J. Colloid Interface Sci.* **2009**, *336* (1), 235−243.
(20) Abate, A. R.; Thiele, J.; Weitz, D. A. One-step Formation of Multiple Emulsions in Microfluidics. *Lab Chip* **2011**, *11* (2), 253−258.
(21) Ren, P. W.; Ju, X. J.; Xie, R.; Chu, L. Y. Monodisperse Alginate Microcapsules with Oil Core Generated from a Microfluidic Device. *J. Colloid Interface Sci.* **2010**, *343* (1), 392−395.
(22) Park, M. J.; Balakrishnan, P.; Yang, S. G. Polymeric Nanocapsules with SEDDS Oil-core for the Controlled and Enhanced Oral Absorption of Cyclosporine. *Int. J. Pharm.* **2013**, *441* (1−2), 757−764.
(23) Blattler, W. A.; Kuenzi, B. S.; Lambert, J. M.; Senter, P. D. New Heterobifunctional Protein Cross-Linking Reagent That Forms an Acid-Labile Link. *Biochemistry* **1985**, *24* (6), 1517−1524.
(24) Wolff, J. A.; Rozema, D. B. Breaking the Bonds: Non-viral Vectors Become Chemically Dynamic. *Mol. Ther.* **2008**, *16* (1), 8−15.
(25) Vaupel, P.; Kallinowski, F.; P, O. Blood Flow, Oxygen and Nutrient Supply, and Metabolic Microenvironment of Human Tumors: A Review. *Cancer Res.* **1989**, *49*, 6449−6465.
(26) Subedi, R. K.; Kang, K. W.; Choi, H.-K. Preparation and Characterization of Solid Lipid Nanoparticles Loaded with Doxorubicin. *Eur. J. Pharm. Sci.* **2009**, *37* (3−4), 508−513.
(27) Walls, Z. F.; Gong, H.; Wilson, R. J. Liposomal Coencapsulation of Doxorubicin with Listeriolysin O Increases Potency via Subcellular Targeting. *Mol. Pharmaceutics* **2016**, *13* (3), 1185−1190.
(28) Ohkubo, S.; Miyadera, K.; Sugimoto, Y.; Matsuo, K.; Wierzba, K.; Yamada, Y. Identification of Substrate Sequences for Membrane Type-1 Matrix Metalloproteinase using Bacteriophage Peptide Display Library. *Biochem. Biophys. Res. Commun.* **1999**, *266* (2), 308−313.
(29) Remacle, A.; Murphy, G.; Roghi, C. Membrane Type I-matrix Metalloproteinase (MT1-MMP) is Internalised by Two Different Pathways and is Recycled to the Cell Surface. *J. Cell Sci.* **2003**, *116* (19), 3905−3916.
(30) Fernandez-Carballido, A.; Pastoriza, P.; Barcia, E.; Montejo, C.; Negro, S. PLGA/PEG-Derivative Polymeric Matrix for Drug Delivery System Applications: Characterization and Cell Viability Studies. *Int. J. Pharm.* **2008**, *352* (1−2), 50−57.

DOI: 10.1021/acsami.6b08994
ACS Appl. Mater. Interfaces 2017, 9, 71−79